

Novel Process for Producing Cubic Liquid Crystalline Nanoparticles (Cubosomes)

Patrick T. Spicer* and Kristin L. Hayden

*The Procter and Gamble Company, Corporate Engineering, 8256 Union Centre Boulevard,
West Chester, Ohio 45069*

Matthew L. Lynch, Akua Ofori-Boateng, and Janet L. Burns

*The Procter and Gamble Company, Corporate Research, 11810 East Miami River Road,
Ross, Ohio 45061*

Received January 31, 2001. In Final Form: June 29, 2001

A novel process for producing cubic liquid crystalline nanoparticles (cubosomes) has been developed. The process entails simple mixing of two waterlike solutions with a minimal input of energy. The key to this process is the inclusion of hydrotrope. Most lipids, such as monoolein, used to form cubic liquid crystals are essentially insoluble in water. The hydrotrope dissolves the lipid to create a waterlike solution. Water is added to the hydrotrope solution, resulting in a precipitous decrease in lipid solubility. Provided that the dilution trajectory falls into a cubic phase–water miscibility gap, nanometer-scale cubic liquid crystalline particles form spontaneously, presumably from a homogeneous nucleation mechanism. The process is versatile enough to accommodate any lipid and hydrotrope combination that forms cubic liquid crystalline material upon dilution. Actives and stabilizers can be formulated into either of the two solutions, allowing the production of colloiddally stabilized, controlled-release dispersions. The phase diagram of the monoolein–ethanol–water system is determined to assess appropriate formulation of solutions and to develop dilution trajectories. This process replaces current processes that require long hold times, processing of solidlike materials, and very high-energy inputs to create cubosome nanoparticle dispersions. This process produces smaller, more stable cubosomes than by conventional bulk dispersion techniques.

Introduction

The self-assembly of amphiphilic molecules (i.e., molecules with hydrophobic and hydrophilic character) into complex phases is a broad and active area of research. Examples of amphiphilic molecules include not only surfactants but also some polymers and polar lipids. Amphiphile phases display a wide range of behaviors, and the past decade has seen a renaissance in the study of their behavior, especially liquid crystalline and microemulsion systems. A fascinating liquid crystalline phase exhibited by amphiphiles is the bicontinuous cubic phase. The bicontinuous cubic phase was first documented by Luzzati et al.,¹ while the model of its geometric structure was later supplied by Scriven.² More recent descriptions of bicontinuous cubic phase structure have required the application of differential geometry and are summarized by Hyde et al.³ The basic building block of the bicontinuous cubic phase is the lipid bilayer. In a cubic phase, lipid bilayers are arranged in periodic three-dimensional structures by contorting the bilayers into the shape of infinite periodic minimal surfaces (IPMS). With such an arrangement, at any place on the surface the average curvature is zero, similar to a saddle. One of the best characterized systems, glycerol monoolein–water, exhibits two main forms of the bicontinuous cubic phase: the gyroid I_{a3d} (low hydration) and the diamond P_{n3m} (high hydration). Figure 1 shows a representation of the

bicontinuous I_{a3d} cubic unit cell from several different perspectives, calculated using the nodal surface approximation to the IPMS.⁴ The surface shown represents the bicontinuous lipid bilayer portion of the cubic phase that is surrounded by the aqueous phase. The bicontinuous arrangement minimizes stress and free energy and produces bicontinuous water and oil domains with an extremely high surface area, on the order of 400 m²/g of cubic phase.⁵ The interconnectedness of the structure results in a clear viscous gel (Figure 2) similar in appearance and rheology to cross-linked polymer hydrogels. However, monoglyceride-based cubic gels possess significantly more long-range order than hydrogels and, because of their composition (i.e., lipid and water), excellent biocompatibility.

The particular properties of monoglyceride-based cubic phases, temperature stability, bicontinuous structure, high internal surface area, solidlike viscosity, and low-cost raw materials, make them desirable for consumer product and pharmaceutical industry applications. The most popular application of cubic phase is as a delivery vehicle for hydrophobic and/or hydrophilic materials that, after solubilization into the cubic gel, diffuse out in a controlled-release manner. Three macroscopic forms of cubic phase are typically encountered: precursor, bulk gel, and particulate dispersions (cubosomes). The precursor form exists as a solid or liquid material that forms cubic phase in response to a stimulus, such as contact with liquid. Bulk cubic phase gel is an optically isotropic, stiff, solidlike material. Cubic gel in equilibrium with water

* Corresponding author e-mail: spicer.pt@pg.com.

(1) Luzzati, V.; Tardieu, A.; Gulik-Kryzwicki, T.; Rivas, E.; Reiss-Husson, F. *Nature* **1968**, *220*, 485.

(2) Scriven, L. E. *Nature* **1976**, *263*, 123–125.

(3) Hyde, S.; Andersson, A.; Larsson, K.; Blum, Z.; Landh, T.; Lidin, S.; Ninham, B. W. *The Language of Shape*, 1st ed.; Elsevier: New York, 1997; Chapter 1.

(4) von Schnering, H. G.; Nesper, R. *Z. Phys. B: Condens. Matter* **1991**, *83*, 407–412.

(5) Lawrence, M. J. *Chem. Soc. Rev.* **1994**, *23*, 417–423.

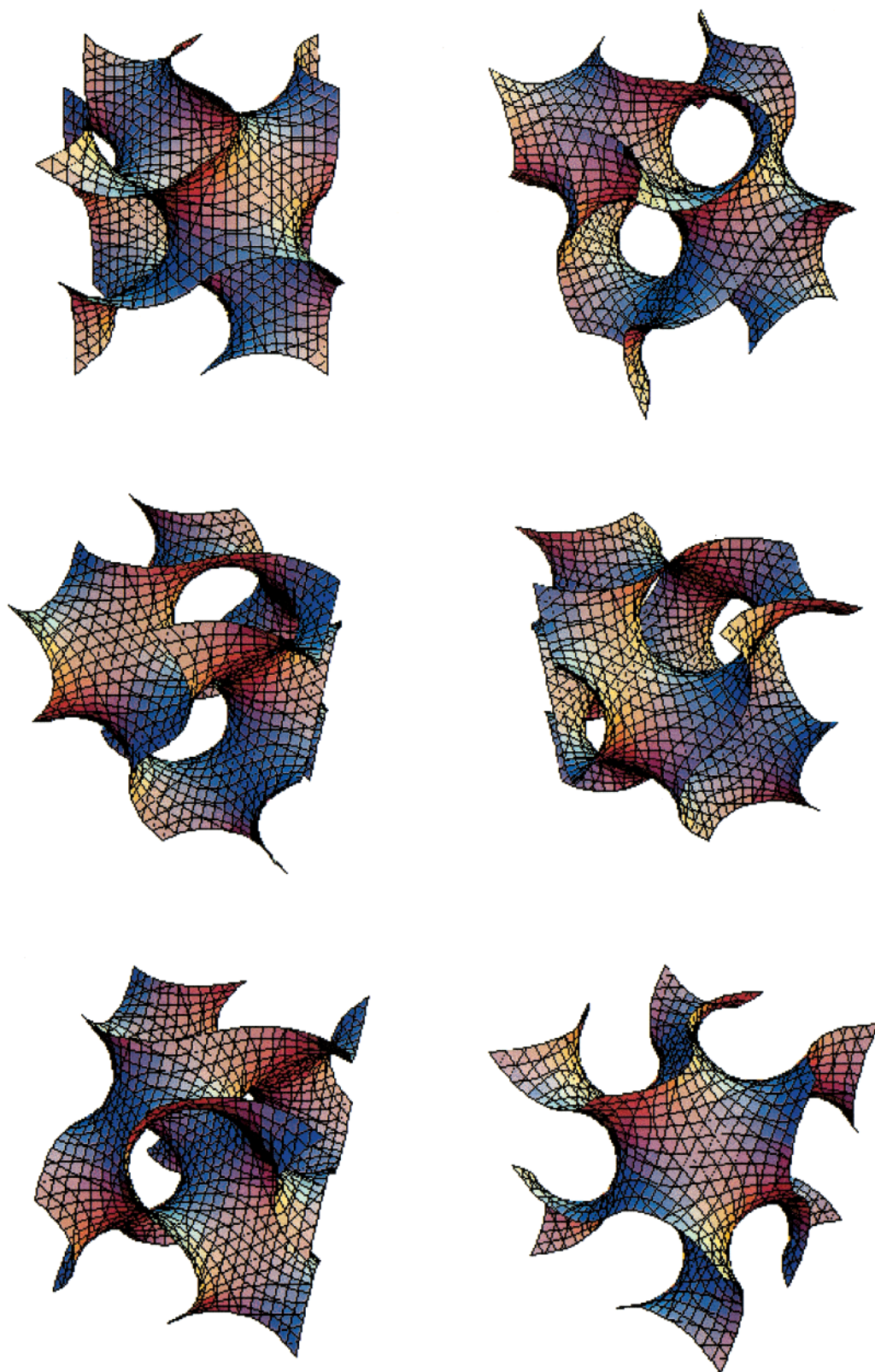


Figure 1. Mathematical representation of the structure of the bicontinuous gyroid I_{a3d} cubic liquid crystalline unit cell (six perspectives of the unit cell are shown). The surface plotted represents the lipid bilayer portion of the cubic liquid crystalline material. The structure of the cubic phase is unique in that it can contain either oil- or water-loving materials in a high surface area, closed environment that allows for controlled release and delivery of active materials.

can be dispersed into particles called cubosomes,⁶ analogous to the formation of vesicles from lamellar liquid crystalline material. A recent review⁷ provides a com-

prehensive summary of active ingredients delivered by cubic phase.

Despite intense interest in cubosome applications, we have found no work examining the practical aspects of large-scale processing and production of cubosomes.

(6) Larsson, K. *J. Phys. Chem.* **1989**, *93*, 7304–7314.

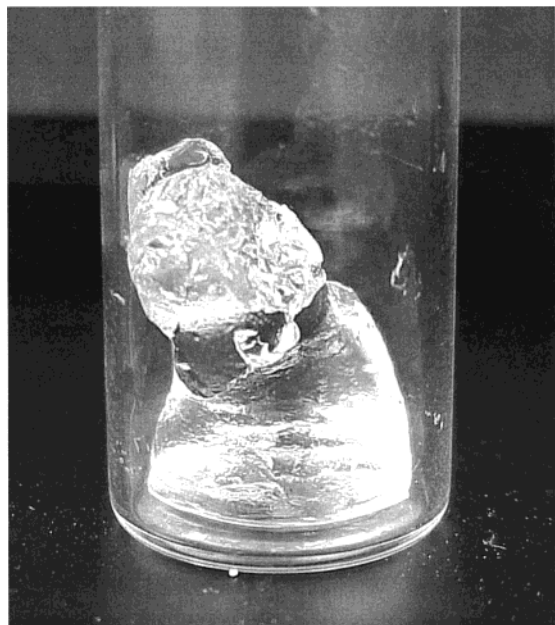


Figure 2. Photograph of a sample of cubic gel. Cubic gel is a clear, high-viscosity gel that does not flow under gravity.

Cubosomes are usually produced by combining monoolein and water at 40 °C for 24 h.⁸ The resultant cubic liquid crystalline gel is dispersed into particles via the application of mechanical or ultrasonic energy. High-pressure homogenizers are often employed to produce cubosomes, requiring high pressures and numerous passes before homogeneous nanoparticle dispersions are produced.⁹ Finally, the cubosomes are stabilized against flocculation by polymer addition. The above process can be difficult to scale-up and, most importantly, runs the risk of degrading the unique cubic structure via excessive energy input. As a result, it is useful to develop a process for producing cubosomes that requires no significant energy input and avoids the intermediate formation of viscous bulk cubic gel. To this end, we study cubic phase formation in the presence of a hydrotrope, defined here as a molecule with hydrophobic and hydrophilic character but incapable of displaying surfactant phase behavior (i.e., micelle formation). Hydrotropes are perversely well-known for their efficiency at disrupting liquid crystalline materials.¹⁰ However, some hydrotropes permit formation of liquid crystalline materials at significant concentrations, suggesting their use as facilitators of dispersed liquid crystalline particle formation. Friberg et al.^{11,12} achieved the formation of lamellar liquid crystalline vesicles by simply diluting a liquid precursor with water. The process formed smaller and more stable vesicles than those formed by traditional high-shear and high-pressure dispersion methods.¹¹ Similarly, the objective of this paper is to explore the spontaneous formation of cubosomes from a hydrotrope solution, avoiding excessive energy input.¹³

(7) Drummond, C. J.; Fong, C. *Curr. Opin. Colloid Interface Sci.* **2000**, *4*, 449–456.

(8) Landh, T.; Larsson, K. GS Biochem AB. U.S. Patent 5,531,925, 1993.

(9) Ljusberg-Wahren, H.; Nyberg, L.; Larsson, K. *Chim. Oggi* **1996**, *14*, 40–43.

(10) Pearson, J. T.; Smith, J. M. *J. Pharm. Pharmacol.* **1974**, *26*, 123–124.

(11) Friberg, S. E.; Campbell, S.; Fei, L.; Yang, H.; Patel, R.; Aikens, P. A. *Colloids Surf., A* **1997**, *129–130*, 167–174.

(12) Friberg, S. E.; Yang, H.; Fei, L.; Sadasivan, S.; Rasmussen, D. H.; Aikens, P. A. *J. Dispersion Sci. Technol.* **1998**, *19*, 19–30.

(13) Lynch, M. L.; Spicer, P. T. The Procter and Gamble Co. U.S. Patent Appl., 2000.

This paper is concerned with the production of cubosomes via novel processing techniques that eliminate the detrimental effects of high-energy input. Ethanol is used as a hydrotrope to create a liquid precursor that, when diluted, forms cubosomes spontaneously. Hydrotropes do not form liquid crystals on their own, but they do exhibit a “salting-in” behavior, increasing the solubility of otherwise water-insoluble lipids such as monoolein. However, the hydrotrope must be present at substantial quantities to exhibit this “hydrotropic” property. So, when diluted, cubic liquid crystalline particles spontaneously form as cubosomes by a presumed homogeneous nucleation process. The ternary phase diagram of the monoolein–ethanol–water system is determined in this work and used as a guide for development of unique processes producing cubosomes via different phase trajectories. Cubic liquid crystalline nanoparticles and microparticles, as well as bulk cubic gel, can be produced using the techniques outlined in this work. The technique also offers the advantage of direct inclusion of active ingredients and colloidal stabilizers. The cubosome processes developed here are unique in that they remove the need for handling waxy solids (i.e., monoolein) and energetic dispersion of bulk solidlike cubic gels.

Experimental Section

Materials. Monoolein was obtained from Grindsted A/S (Dimodan MO90K, Denmark) and was determined by gas chromatography to be greater than 90% pure. There were minor fractions of diglycerides, triglycerides, and a monostearin glycol. Ethanol was purchased from Aldrich and was 99% pure. All water was deionized using Millipore Water systems. Poloxamer 407 (PEO₉₈PPO₆₇PEO₉₈) with an average formula weight of 12 500 was purchased from Spectrum (P1126). Sonication of the liquid crystalline material was carried out using a Misonix Sonicator XL Probe, and high-shear experiments were performed using an Ika model T50 rotor stator mill operated at 10 000 rpm. All measurements and processing were carried out at 25 °C unless otherwise noted.

Cryo-Transmission Electron Microscopy (Cryo-TEM). Samples were prepared in a controlled environment vitrification system (CEVS) as described by Bellare et al.¹⁴ In particular for this work, a 3- μ L drop of solution was placed on a carbon-coated porous-polymer support film mounted on a standard 300-mesh TEM grid (Ted Pella, Inc.). The drop was blotted with filter paper until it was reduced to a thin film (10–200 nm) spanning the holes (2–8 μ m) of the support film. The sample was then vitrified by rapidly plunging it through a synchronous shutter at the bottom of the CEVS into liquid ethane at its freezing point. The vitreous specimen was transferred to a Philips CM120 transmission electron microscope for imaging using a Gatan cryo-holder. The temperature of the sample was kept under –170 °C throughout the examination. Specimens were examined in the low-dose imaging mode at 120 kV, and images were recorded digitally by a Gatan 791 MultiScan CCD camera using Digital Micrograph 3.3 software.

Small-Angle X-ray Scattering (SAXS). SAXS was performed on samples with Cu K α radiation ($\lambda = 0.154$ nm) generated with a Rigaku RU-300 rotating anode. The generator was operated at 40 kV and 40 mA with a 0.2 \times 0.2 mm focal size (a 0.2 \times 2 mm filament run in point mode). The patterns were collected with the Siemens two-dimensional small-angle scattering system, which consists of the HI-STAR wire detector and Anton Parr HR-PHK collimation system. Collimation is achieved with a single 100 mm diameter pinhole, 490 mm from the focal spot. The size of the focal spot restricts beam divergence. A 300- μ m guard pinhole is placed 650 mm from the focal spot, just in front of the sample. The detector is placed a distance of 650 mm from the sample. Ni filters were used to eliminate the K β radiation. Because of the small beam size and large sample-to-

(14) Bellare, J. R.; Davis, H. T.; Scriven, L. E.; Talmon, Y. *J. Electron Microsc. Tech.* **1988**, *10*, 87–111.

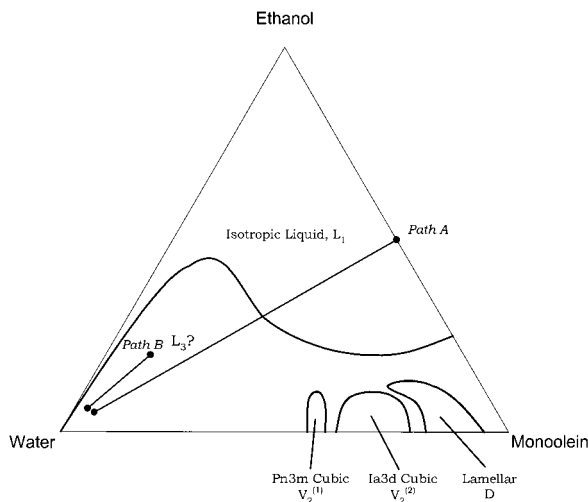


Figure 3. Ternary phase diagram for the monoolein–ethanol–water system. The system exhibits five single-phase regions, including four liquid crystalline phases, despite significant levels of ethanol hydrotrope. The large region of isotropic liquid provides broad flexibility for the formulation of precursors forming cubic gel and cubosome dispersions upon dilution.

detector distance, two-dimensional profiles can be obtained with a minimum of instrumental smearing, so no smearing corrections were employed.

Particle Size Distribution (PSD). Determination of the PSD of the cubosome dispersions was carried out using focused beam reflectance measurement (FBRM; Lasentec, Redmond, WA) to characterize particles larger than 1 μm and dynamic light scattering (DLS; Brookhaven, NY) to characterize submicron particles. FBRM analysis was performed on cubosome dispersions in a sample beaker stirred at 100 rpm and allowed characterization of concentrated dispersions as a result of the rapid rotation of the optics in the Lasentec sample probe. DLS experiments were performed on a Brookhaven light scattering system. Samples were diluted and then filtered using a 1- μm syringe filter (Syrfil MF, Corning) to remove any particles larger than 1 μm . The system uses an 8-W water-cooled Ar-ion laser (Lexel) with a wavelength of 514.5 nm, and all runs were performed at a laser power of 100 mW and a scattering angle of 90°. Sample cells were placed in a temperature-controlled vat containing index-matching Decalin fluid and kept at 25 °C, and the appropriate value of the viscosity of water was used in all calculations. The CONTIN software routine was used to extract a PSD from the measured autocorrelation functions.

Results and Discussion

Monoolein–Ethanol–Water Phase Diagram. The ternary phase diagram for the monoolein–ethanol–water system (Figure 3) was constructed by first characterizing binary component mixtures, followed by making strategic ternary mixtures to define the limits of the phase regions. Literature binary phase diagrams of monoolein–water^{15,16} were confirmed by conventional and DIT¹⁷ phase study methods. Our data were in excellent agreement with literature results. Ethanol and water are known to be totally miscible. The miscibility of monoolein in ethanol was determined by adding enough ethanol to totally dissolve the monoolein. The phase boundaries in the ternary system were determined by making ternary mixtures, equilibrating for 30 days, and extrapolating data to the edges of the triangle (binary data). No surfactant degradation-related phase changes were observed during

the equilibration period.¹⁸ Phases were classified by appearance, rheology, optical properties (e.g., optical birefringence), and literature references. All characterization was carried out at 25 °C unless otherwise noted.

The system exhibits four single-phase regions: L_1 (isotropic liquid), $V_2^{(1)}$ – P_{n3m} (P_{n3m} diamond bicontinuous cubic liquid crystalline), $V_2^{(2)}$ – I_{a3d} (I_{a3d} gyroid bicontinuous cubic liquid crystalline), and D (lamellar liquid crystalline). Remarkably, the three liquid crystalline regions extend as high as 10% ethanol. The addition of hydrotrope is generally thought to “destroy” liquid crystal at relatively low levels.¹⁰ Two other published phase diagrams are known for this ternary system. The diagram proposed by Leng and Parrott¹⁹ is inconsistent with respect to the published binary monoolein–water phase diagram, and the diagram proposed by Engstrom et al.²⁰ is partially consistent but incomplete. Neither indicates the presence of the miscibility gap necessary to fabricate cubosomes. Of particular significance is the $V_2^{(1)} + L_1$ region to the left of the $V_2^{(1)}$ region. It is in this region that cubic phase dispersion (also known as cubosomes) can be fabricated, as cubosomes are merely cubic liquid crystalline material in equilibrium with L_1 . In the middle left portion (low monoolein base) of the ternary phase diagram is a two-phase region exhibiting a binary mixture of lean and rich isotropic liquid. This is reminiscent of the liquid–liquid miscibility gaps exhibited by ethoxylated surfactants.²¹ The emulsions exhibit apparently low interfacial tension, remain stable indefinitely, and form spontaneously upon dilution of isotropic liquid into the two-phase region. Furthermore, Engstrom et al.²⁰ report a sponge (L_3) phase in the small region labeled “ $L_3?$ ” in Figure 3. The region is characterized by a distinct bluish tint that is also observed in our samples. However, for our samples, the bluish tint disappears upon equilibration. This is inconclusive as the sponge phase is often difficult to delineate because of the sometimes long-time kinetics associated with its formation.²² The possible existence of an L_3 phase in our system is worth noting, however, as it has been suggested that cubosomes often form in a three-phase (i.e., $L_3 + V_2^{(1)} + L_1$) region. Such a region could exist in a triangle drawn between the water apex, the top left edge of the $V_2^{(1)}$ region, and the lower edge of the L_3 region suggested by Engstrom et al.²⁰ We, however, have only observed cubosomes in the two-phase region between the water apex and the left edge of the $V_2^{(1)}$ region.

Cubosomes from Pseudo-Binary Systems. Cubosomes were first made in a pseudo-binary system of monoolein–water (including polymer at low levels) using the conventional technique of energetic dispersion of bulk cubic gel.⁸ Melted Poloxamer 407 (8% w/w) and monoolein (92% w/w) were combined to form a homogeneous solution. The monoolein–polymer solution was then added to deionized water to form a 1.8% mixture of monoolein containing 98% water and 0.2% Poloxamer 407. The mixture was sonicated for 60 min in a controlled temperature ultrasonic bath, maintained at 25 °C, to disperse the cubic liquid crystalline gel. Cryo-TEM (Figure 4) revealed mostly square cubosomes that were about 100–

(18) Caboi, F.; Amico, G. S.; Pitzalis, P.; Monduzzi, M.; Nylander, T.; Larsson, K. *Chem. Phys. Lipids* **2001**, *109*, 47–62.

(19) Leng, F. J.; Parrott, D. T. Chesebrough-Pond’s USA Co. U.S. Patent 5,593,663, 1997.

(20) Engstrom, S.; Alfons, K.; Rasmusson, M.; Ljusberg-Wahren, H. *Prog. Colloid Polym. Sci.* **1998**, *108*, 93–98.

(21) Sjoblom, J.; Stenius, P.; Danielsson, I. In *Nonionic Surfactants: Physical Chemistry*; Schick, M., Ed.; Marcel Dekker: New York, 1993; p 369.

(22) Penders, M. H. G. M.; Strey, R. *J. Phys. Chem.* **1995**, *99*, 6091–6095.

(15) Laughlin, R. G. *The Aqueous Phase Behavior of Surfactants*, 1st ed.; Academic Press: New York, 1994.

(16) Briggs, J.; Chung, H.; Caffrey, M. *J. Phys. II* **1996**, *6*, 723–751.

(17) Laughlin, R. G.; Lynch, M. L.; Marcott, C.; Munyon, R. L.; Marrer, A. M.; Kochvar, K. A. *J. Phys. Chem. B* **2000**, *104*, 7354–7362.

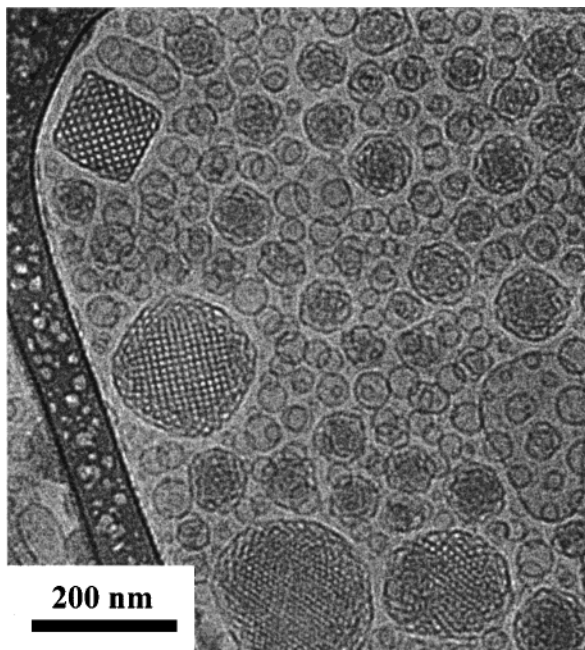


Figure 4. Cryo-transmission electron micrograph of dispersed particles of cubic liquid crystalline material or cubosomes. The cubosomes are approximately 150 nm in diameter and are composed of hundreds of the unit cells represented in Figure 1. Also visible are numerous vesicles.

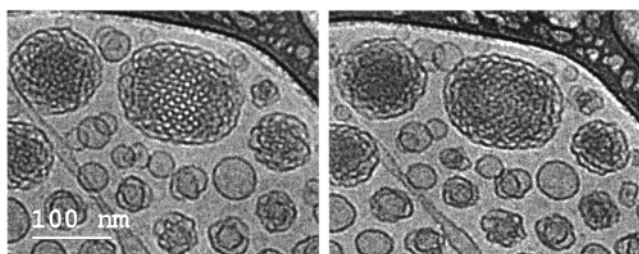


Figure 5. Stereographic images of a cubosome rotated 0 and 15° from the normal. The rotation causes a blurring of the well-defined cubic lattice but does not increase the edge length appreciably.

300 nm along an edge. The unit cell structure is evident from alternating water (light gray dots) and oil channels (dark matrix). Fourier analysis of the periodicity results in 150 Å, which is consistent with SAXS for monoolein–water cubic phases.²³ The three-dimensional shape of the aggregates, however, is elusive. Stereographic images taken at 0 and 15° from the normal (Figure 5) show some blurring in the well-defined matrix of water channels from visualizing successive layers below the top layer. However, the length of the particle edge does not change upon tilting. This is peculiar because rotating a cube by 15° should result in an increase of 22% in size²⁴ along the direction of rotation. This suggests that the aggregate might be more spherulike or relatively flat, although more distinctly cubic cubosome aggregates have been documented.²⁵

Cubic Liquid Crystalline Phase in the Presence of Hydrotrope. Cubosomes were also formed in the presence of significant levels of hydrotrope by sonication-based methods. Bulk cubic gel was fabricated by the combination of molten monoolein (93% w/w) and ethanol

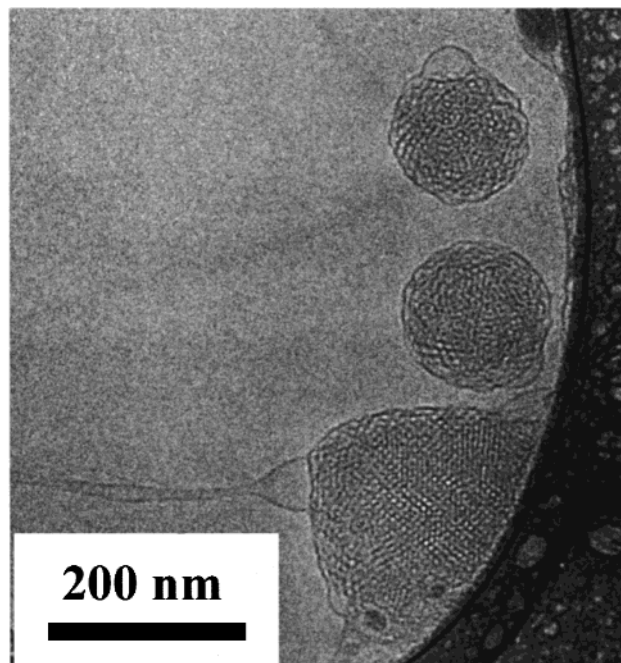


Figure 6. Cryo-TEM image of cubosomes formed by sonicating bulk cubic gel containing ethanol hydrotrope. Despite the presence of 5% ethanol, bulk cubic gel is formed, and cubosome particles form upon energetic dispersion.

(7% w/w) to form a low-viscosity isotropic liquid. A 1.2% Poloxamer 407 solution was added to the liquid, forming a viscous, cubic liquid crystalline gel in the presence of excess water (final composition: 68% monoolein, 26.7% water, 5% ethanol, and 0.3% Poloxamer 407). The mixture was sonicated for 5 min. Figure 6 shows cryo-TEM photographs of two cubosomes about 200 nm in diameter. These cubosomes are similar in size and shape to those formed without ethanol, although more circular than square. The cubosomes in Figure 6 possess a more disordered structure than those in Figure 4 and may not have fully crystallized into cubosomes, resembling the “...folded structures with numerous interlamellar connections...” shown in Figure 14 of Almgren et al.²⁶ Also visible is a larger region of cubic liquid crystal attached to the support and displaying a well-defined cubic lattice. The larger pieces of cubic gel form as a result of incomplete dispersion by the short application of ultrasonic energy, this dispersion was macroscopically more opaque than that shown in Figure 4 (a dispersion formed after 60 min of sonication). Large amounts of energy per unit volume are clearly necessary to completely disperse the cubic gel into cubosome nanoparticles when starting from bulk cubic gel. Finally, note that both cubosomes in Figure 6 have a hemispherical-shaped vesicle extending from an edge. The formation of a vesicular coating on cubosomes has been suggested as a thermodynamic means of avoiding exposure of lipid hydrocarbon chains as the cubic liquid crystalline gel is fragmented during dispersion.⁹

Formation of cubic liquid crystals in the presence of hydrotrope was confirmed by SAXS measurements on ethanol-containing cubic phase gels. SAXS measurements were made on cubic phase gels of 2% ethanol (i.e., 50% monoolein, 48% water, and 2% ethanol) and compared to those without ethanol (i.e. 50% monoolein and 50% water). Similar results were observed for 8% ethanol (Table 1). The SAXS data showed only those lines that were expected

(23) Qiu, H.; Caffrey, M. *Biomaterials* **2000**, *21*, 223–234.

(24) From $d_\theta/d_{15^\circ} = (\sin \theta + \cos \theta)$ where d is the distance measured on the image and θ is the angle of rotation.

(25) Gustafsson, J.; Ljusberg-Wahren, H.; Almgren, M.; Larsson, K. *Langmuir* **1997**, *13*, 6964–6971.

(26) Almgren, M.; Edwards, K.; Garlsson, G. *Colloids Surf., A* **2000**, *174*, 3–21.

Table 1. SAXS Data for P_{n3m} Cubic Phase Gels

Miller index of reflection	d_{hkl}/d_{110}		
	50% monoolein		Winey et al. ²⁷ and Funari and Gert ²⁸ P _{n3m} cubic phase
	48% water 2% ethanol (w/w)	50% monoolein 50% water (w/w)	
110	1.00	1.00	1.00
111	0.819	0.816	0.816
200	0.707	0.704	0.707
211	0.574	0.573	0.577
220	0.495	0.496	0.500

for P_{n3m} symmetry.^{27,28} The cell parameter was calculated from the slope of a plot of d_{hkl} vs $(h^2 + k^2 + l^2)^{-1/2}$ and determined to be 109.8 and 107.9 Å, respectively, which is well within the bounds reported by Qiu and Caffrey.²³ Consequently, it is proven that the cubic phase can exist in the presence of hydrotrope.

Making Cubosomes by Nucleation. The dilution (nucleation) process provides the ability to produce cubosomes without laborious fragmentation. The best way to anticipate appropriate dilution pathways is by charting trajectories on the ternary diagram. Dilution with water is essentially equivalent to drawing a line from some composition to the water apex (Figure 3). Of course, phase diagrams speak to thermodynamic properties; dilution has a large kinetic component so that this is an approximation. The phase diagram also offers a means of determining the yield of cubic phase obtained by a dilution process using the tie lines between the isotropic liquid and the cubic phase in conjunction with the Lever Rule.

One of the most logical dilution paths is from the large isotropic L₁ region because the isotropic liquid is low viscosity and conveniently mixed with water. Consider that path A (Figure 3) represents the dilution of an isotropic liquid (50% monoolein, 50% ethanol) with a polymer–water solution to form a colloidal dispersion of cubosomes in water (89% water, 5% monoolein, 5% ethanol, and 1% Poloxamer 407). Cubosomes form spontaneously with minimal energy input other than that required to contact the two liquids and, literally, gentle mixing by hand inversion of the container. The dispersions are estimated to be 10% cubosomes dispersed in 90% liquid (mostly water). A small amount of polymer is necessary to stabilize the particles against flocculation; the presence of this small amount of polymer does not alter the phase behavior of the system. Without the polymer, the cubosomes will flocculate quite rapidly, on the order of seconds. Cubosomes made by our process (with added polymer) show excellent long-term stability despite the relatively low polymer content. Cubosome dispersions prepared by dilution of isotropic liquid were stable against flocculation for at least 6 months with only 1% polymer present. This is in agreement with the work of Friberg et al.,¹¹ who found that vesicles formed via dilution were more stable than those formed by energy-intensive methods. In contrast, Gustafsson et al.²⁵ required much higher polymer concentrations (i.e., 4–12%) to stabilize cubosomes for several months as prepared by high-pressure homogenization. Although speculative, the mechanism for the superior stability of dilution-produced cubosomes is likely the more homogeneous distribution of the stabilizing polymer to the cubosome surfaces during nucleation than during energetic dispersion.

Cryo-TEM images of the dispersion made by dilution path A are shown in Figure 7. Figure 7a shows a cubosome

about 300 nm in diameter with a lamellar vesicular surface coating. These cubosomes are similar in appearance and structure to those previously noted. It is worth emphasizing that this process creates nanoparticles of cubic liquid crystalline gel without any significant mechanical energy input. It is likely that a phase inversion process occurs as the dilution path crosses the isotropic liquid phase boundary (Figure 3). As a result, interfacial energy is applied instead of mechanical energy toward the dispersion of the cubic gel that forms. On a practical scale, some adjustment of the PSD will likely be needed, but the total energy input will be much less than that needed to disperse bulk cubic gel “from scratch”. Finally, in all of the cryo-TEM images shown thus far, some vesicles are always present with the cubosomes. Recalling that trajectories do not reflect kinetic phenomenon, Figure 7b,c shows transitional vesicle structures (indicated by the arrows) formed during the dilution. It is believed that these vesicles are precursors for cubosomes^{25,29} and that the remaining vesicles will transform into cubosomes rapidly. More conclusive research into this question is warranted, but the structures in Figure 7b,c are reminiscent of the structures formed by membrane fusion of phospholipid vesicles during their phase transition to the hexagonal phase.³⁰

Dilution from the emulsion region provides an interesting contrast (path B, Figure 3) to dilution of an isotropic liquid. Emulsions are excellent precursors for cubosome dispersions because they can be easily dispersed and stabilized prior to cubosome formation to prevent liquid crystal degradation and agglomeration, respectively. In general, the low-viscosity emulsions formed in this region are promising cubosome precursors because their PSD is easily tailored by low shear, stabilized, and finally diluted into the cubic liquid equilibrium region to form cubosomes. A macroemulsion was first prepared (70% water, 20% ethanol, and 10% monoolein) and then diluted with Poloxamer 407 solution to form a cubic liquid dispersion (90% water, 6% ethanol, 3% monoolein, and 1% polymer) using only mild hand agitation.

Cubosome nanoparticles (100–300 nm in diameter) were again formed spontaneously during the emulsion dilution process, as verified by cryo-TEM imaging. Because the cubosome particles were formed from a macroemulsion without any application of shear beyond hand mixing, there appears to be a broader PSD than that produced by dilution from the L₁ region (direct nucleation process). In addition to nanoparticles, particles on the order of micrometers were also observed. Figure 8 shows a differential interference contrast micrograph (with and without crossed polarizers) of one of these larger cubosomes. The longest dimension is about 7 μm along the edge. Surprisingly, the particles possess a distinct cubic shape despite their nonsolid state and their large scale relative to the cubic unit cell dimensions, reminiscent of previously reported cubic phase-containing emulsions.³¹ These particles are clearly formed with edges that terminate along the principal directions of the unit cell.²⁵ While Figure 8 confirms the presence of particles with distinct cubic morphology, it also shows via polarized light microscopy the existence of a birefringent, probably lamellar, surface coating on the particles in agreement

(29) Siekmann, B.; Bunjes, H.; Koch, M. H. J.; Carlson, T.; Westesen, K. *Proc. Int. Symp. Controlled Release Bioact. Mater.* **1997**, *24*.

(30) Talmon, Y.; Burns, J. L.; Chestnut, M. H.; Siegel, D. P. *J. Electron Microsc.* **1990**, *14*, 6–12.

(31) Lynch, M. L.; Kochvar, K. A.; Burns, J. L.; Laughlin, R. G. *Langmuir* **2000**, *16*, 3537–3542.

(27) Winey, K. I.; Thomas, E. L.; Fetters, L. J. *J. Chem. Phys.* **1991**, *95*, 9367–9375.

(28) Funari, S. S.; Rapp, G. *J. Phys. Chem. B* **1997**, *101*, 732.

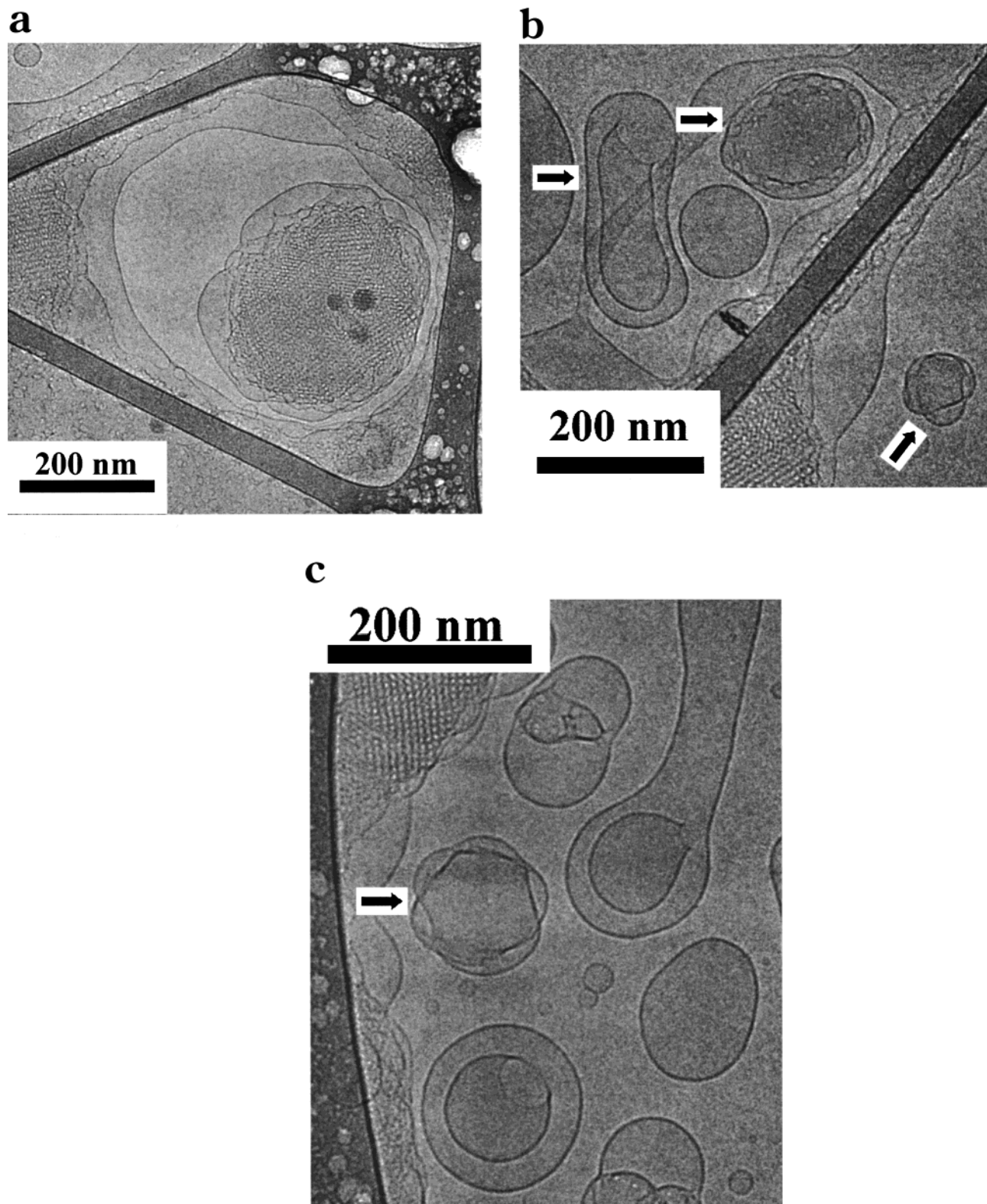


Figure 7. (a) Cryo-TEM image of cubosome nanoparticle formed by dilution of a precursor following dilution path A shown in Figure 3. The cubosomes formed exhibit a similar morphology to those in Figures 4 and 6. (b and c) Transitional vesicles that may be a precursor to cubosomes as equilibrium is approached.

with Gustafsson et al.²⁵ and our results for smaller cubosomes.

Particle Sizing of Cubosomes. Because the PSD of the cubosome dispersions tends to span several decades, two techniques were used for characterization of the PSD: FBRM was used to characterize cubosome particles larger than 1 μm , and DLS was used to measure the submicrometer PSD. FBRM data are presented in the

PSD function. This is a measure of the number concentration of particles, $dN(d_p)$, normalized by the width of the size class containing the particles, $d(d_p)$.³² The FBRM technique returns a chord length (a measure of particle diameter) and allows characterization of dense, opaque

(32) Friedlander, S. K. *Smoke, Dust, and Haze*, 2nd ed.; Wiley: New York, 2000.

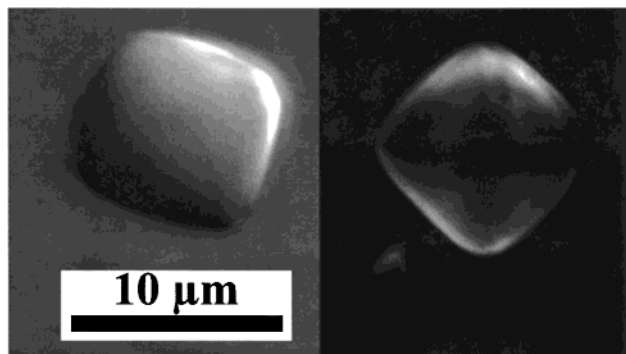


Figure 8. Optical micrograph, with (right) and without (left) crossed polarizers, of macroscopic cubic gel particles produced by dilution of a macroemulsion following dilution path B in Figure 3. Despite the relatively large size of the particles (about $5\ \mu\text{m}$ at their longest), their cubic shape is maintained. Polarized light microscopy reveals the optically birefringent (possibly vesicular) surface coating of the cubosomes, similar to the submicrometer particles in Figures 4, 6, and 7.

slurries but can create false fine readings as a result of the effect of particle shape and orientation on the size measurement. Because the FBRM provides a direct measure of particle size, it is possible to estimate the particle number concentration and determine the relative mass of the cubic phase above (and by mass balance, below) $1\ \mu\text{m}$ in size. DLS does not provide a direct particle measurement but rather a PSD deconvoluted from the autocorrelation function of the scattered light intensity. Each technique is derived from different physical properties, so absolute comparison of the measurements is difficult, and data are presented individually for each technique.

The PSD comparison of dilution-based methods vs energetic-based methods demonstrates that the dilution-based process is far more efficient at generating small particles. Figure 9a compares the cubosome PSDs produced by dilution from the L_1 region to those produced by the energetic dispersion of bulk cubic gel. For this study, high-shear rotor stator mixing was used as the dispersion technique rather than ultrasonic dispersion because it is more easily scaled up and theoretically modeled. All samples had the same final concentration (15%) of cubic liquid crystal. Figure 9a illustrates that energetic dispersion of bulk cubic gel produces the largest particles, producing $3\times$ as many particles greater than $1\ \mu\text{m}$ in size, reflected in the larger magnitude of the size distribution function in Figure 9a. The application of additional shear with a rotor stator during L_1 dilution produces $10\times$ fewer particles larger than $1\ \mu\text{m}$ as compared to hand mixing. Figure 9b shows the intensity-based PSDs measured by DLS for the same three cases shown in Figure 9a. Figure 9b characterizes the relative amounts of particles smaller than $1\ \mu\text{m}$ and is in good agreement with the results in Figure 9a. Hand mixing appears to produce the least submicrometer particles (250–900 nm), consistent with the fact that it is the lowest shear process. Nevertheless, dispersion of the bulk gel using the rotor stator produces a similar PSD extending from 150 to 900 nm. The most nanoparticles are clearly produced by combining the shear and the dilution process, as cubosomes ranging from essentially 100 to 500 nm are produced with the bulk of them around 150 nm (Figure 9b). Siekmann et al.²⁹ used DLS to compare bulk cubic gel dispersion processes and found little difference between high-shear, ultrasonic, and impeller systems but did not measure particle sizes above $1\ \mu\text{m}$ or investigate hydrotrope effects.

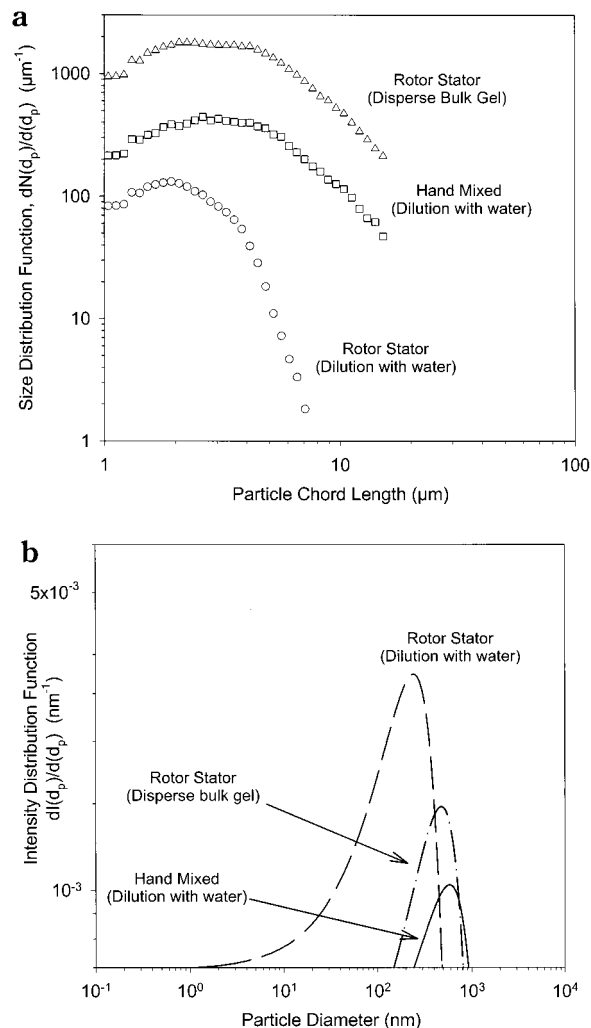


Figure 9. Cubosome PSD as determined by (a) FBRM and (b) DLS. Creation of cubosomes by the conventional technique of high-shear dispersion of bulk cubic gel produces the largest cubosomes, followed by hand mixing and shearing of an isotropic liquid during dilution.

The use of ethanol (or, more generally, hydrotrope) appears to be the key to generating a smaller PSD. Ethanol allows the dissolution of monoolein into isotropic liquid, reducing the operative viscosity significantly. Cubosomes are formed by homogeneous nucleation during the dilution of isotropic liquid, just as the addition of a nonsolvent can be used to induce solid precipitation. The dilution process is thus analogous to the use of precipitation processes to produce nanoparticles, while the conventional bulk gel dispersion technique is more analogous to the attrition of bulk solids. Homogeneous nucleation may be the most desirable process from a nanoparticle production and scale-up perspective, although it can be difficult to precisely control. The hydrotrope also aids processing by creating phase boundaries that, when crossed during dilution, lend interfacial energy to the dispersion process and enable even low-shear hand mixing to produce cubosome nanoparticles. In fact, the dilution process also appears to increase the impact of the high-shear rotor stator as smaller particles are produced using the dilution process than by bulk gel dispersion. Preliminary observations indicate that ethanol affects the viscosity of the bulk cubic gel and may therefore also aid in dispersion by reducing the energy input necessary to reduce particle size. We are currently investigating the rheological behavior of the monoolein–ethanol–water system.

Conclusions

The presence of hydrotrope in the monoolein–water system has led to some unexpected results. First, cubic liquid crystal can be formed at relatively large (i.e., $\leq 10\%$) ethanol levels. This was confirmed by both cryo-TEM techniques on cubic liquid crystal dispersions and SAXS measurements on the bulk cubic phase gel. Second, a more precise look at the monoolein–water–ethanol ternary phase diagram suggests a miscibility gap between L_1 and cubic phase region. Within this region, stable dispersions of cubic liquid crystal or cubosomes form. These results are not unique to ethanol but work with other hydrotropes as well.¹³ Dilution of monoolein–water–hydrotrope mixtures can produce particles as small as 50 nm or as large as 20 μm . The addition of small amounts of shear during the dilution process can be far more efficient than the relatively high shear needed to disperse bulk cubic gel samples. The cubosome dispersions can be stabilized against flocculation during the dilution step, and incorporation of active materials for subsequent delivery can be performed prior to cubosome formation.

Comparisons were made, using PSD measurements, of the dilution process to conventional cubosome processes

involving high-energy dispersion of bulk cubic gel. The dilution process was found to consistently produce smaller, more stable cubosomes with lower energy input than high-shear treatment of bulk cubic gel, which runs the risk of degrading the cubic liquid crystalline structure. The dilution process allows for easier scale-up of a cubosome process and avoids bulk solids handling as well as potentially damaging high-energy input processes. More work is needed to better understand the physical and interfacial effects of the hydrotrope on the cubic liquid crystalline bulk properties in order to design full-scale cubosome processes.

Acknowledgment. We gratefully acknowledge illuminating discussions with Prof. Stig Friberg (Clarkson University, retired) and Prof. Eric Kaler (University of Delaware). We are also grateful to Jeff Grothaus (Corporate Research Division, The Procter and Gamble Company) for X-ray analysis as well as Seth Lindberg and Dirk Domaschko (Corporate Research Division, The Procter and Gamble Company) for additional microscopy.

LA010161W